Supporting Information for:

Structure of Aqueous H_3BO_3 Solutions by DFT and Neutron Scattering

Yongquan Zhou[a,*], Toshio Yamaguchi[b], Wenqian Zhang[a], Kazutaka Ikeda[c], Koji Yoshida[b], Fayan Zhu[a], Hongyan Liu[a]

[a] *Key Laboratory of Comprehensive and Highly Efficient Utilization of Salt Lake Resources; Key Laboratory of Salt Lake Resources Chemistry of Qinghai Province; Qinghai Institute of Salt Lakes, Chinese Academy of Sciences, Xining 810008, China*

[b] *Department of Chemistry, Faculty of Science, Fukuoka University, 8-19-1 Nanakuma, Jonan, Fukuoka 814-0180, Japan*

[c] *High Energy Accelerator Research Organization (KEK), Tsukuba, Ibaraki 305-0801, Japan*

All correspondence should be sen to: Dr. Yongquan Zhou,

E-mail. yongqzhou@163.com

1. Sample Information

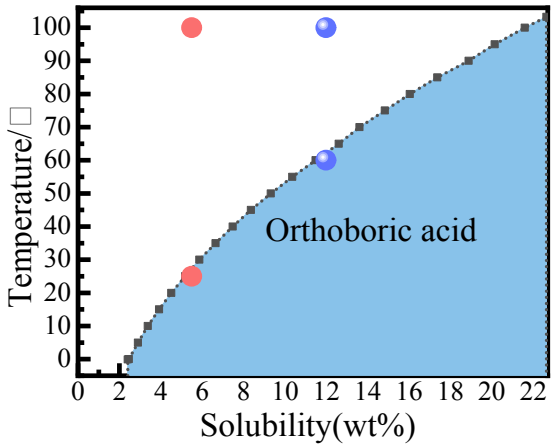

Fig. S1. Sample solutions lay in the H_3BO_3-D_2O binary

(Based on data from Nies, N. P, *et al. J. Chem. Eng. Data*, 1967, 12 (3), 303-313.[1])

In the present work, the deuterated compounds were used to avoid the large incoherent scattering-cross section of H (σ_i^H=82.03 barns and σ_i^D=2.05 barns). Meantime, ^{11}B were used to over come the large absorption of natural boron ($\sigma_a^{natural}B$ = 767.8 barns and $\sigma_a{}^{10}B$ = 0.0055 barns).

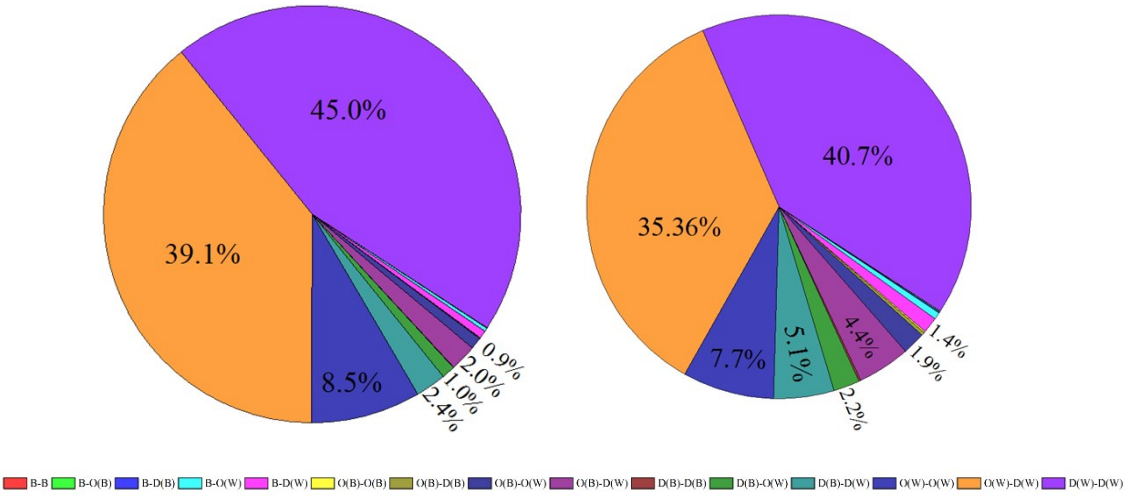

Fig. S2. The contribution of each atom pair to the totall scarttering indensity for aqueous $^2H_3{}^{11}BO_3$ solutions at different concentration (WSR=57, left and WSR=24, right) by nuetron diffraction with λ of 1.798 Å.

2. Parameters for EPSR

Table S1. Bond lengths and angles for describing the simulation molecules

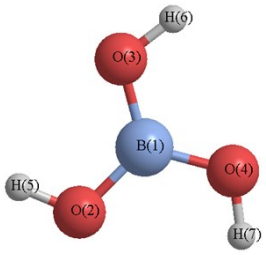

H_3BO_3

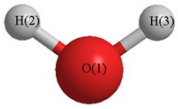

H_2O

Bonds/Å			Angle/°			
atom 1	atom 2	distance	atom 1	atom 2	atom 3	Angle
O(4)	H(7)	0.965	H(7)	O(4)	B(1)	112.652
O(3)-	H(6)	0.965	H(6)	O(3)	B(1)	112.601
O(2)	H(5)	0.965	H(5)	O(2)	B(1)	112.480
B(1)	O(4)	1.367	O(4)	B(1)	O(3)	120.045
B(1)	O(3)	1.367	O(4)	B(1)	O(2)	119.997
B(1)	O(2)	1.367	O(3)	B(1)	O(2)	119.958
O(1)	H(2)	0.956	H(2)	O(1)	O(3)	105.112
O(1)	H(3)	0.956				

Table S2. Potential parameter values for EPSR modelling

	B[2]	O(B) [2]	D(B) [2]	O(W)[3]	D(W)
ε /kJ.mol^{-1}	0.142	0.666	0.00	0.650	0.000
σ/Å	3.528	2.851	0.00	3.160	0.00
Mass	10.810	15.9994	2.000	16.00	2.00
Charge	0.474	-0.368	0.210	-0.8476	0.4238

Table S3. EPSR simulation setup details.

Simulation box	# water molecules	#$B(OH)_3$ molecules	Density /atoms Å^{-3}	Box side length /Å	Iterations times
B57W-298	1000	18	0.09947	31.5572	20100
B57W-373	1000	18	0.09583	31.9518	25414
B57W-343	1000	41	0.09754	32.3002	21362
B57W-373	1000	41	0.09570	32.5057	23843

3.DFT Calculations

Table S4:Calculated conformational populations (p_i, %), energy parameters and bond parameters of $2B(OH)_3 \cdot 6H_2O$ conformers at ωb97xd/6-311++g(2df,2pd) basis level.

isomers		p_i	Bond parameters/Å					ΔG_{PCM}^{inter}	Relative energy
			Intra-B-O	$B\text{-}O_{(W,\ Dual)}$	$B\text{-}O_{(W,\ Don.)}$	$B\text{-}O_{(W,\ Acc.)}$	B-B	kcal/mol	
HB2W6A	MCMP-L	0.000	1.368	3.214	3.352	3.657	4.398	-15.56	8.88
HB2W6B	MCMP-A	24.683	1.367	3.217	3.543	3.712	4.444	-24	0.44
HB2W6C	SMP-A	13.028	1.367	/	3.608	3.785	6.626	-23.62	0.82
HB2W6D	SMP-D	0.001	1.367	3.192	3.576	3.704	5.69	-18.12	6.32
HB2W6E	MCMP-O	0.000	1.368	3.241	3.643	3.667	4.465	-14.83	9.61
HB2W6F	MCMP-E	0.013	1.367	3.326	3.501	3.622	4.343	-19.53	4.91
HB2W6G	BCMP-C	0.452	1.366	/	3.456	3.696	4.016	-21.63	2.81
HB2W6H	PSMP-B	0.007	1.368	3.221	3.498	3.732	3.676	-19.12	5.32
HB2W6I	MCMP-D	0.033	1.366	/	3.503	3.66	4.645	-20.09	4.35
HB2W6J	MCMP-F	0.01	1.367	3.221	3.554	3.643	4.744	-19.38	5.06
HB2W6K	PSMP-D	0.000	1.369	3.229	3.543	3.959	3.372	-15.83	8.61
HB2W6L	BCMP-F	0.003	1.367	3.152	3.528	3.475	4.04	-18.63	5.81
HB2W6M	SMP-B	4.402	1.367	3.2	3.598	3.756	6.157	-22.98	1.46
HB2W6N	MCMP-C	0.085	1.367	3.219	3.575	3.847	4.844	-20.64	3.80
HB2W6O	BCMP-G	0.000	1.367	3.223	3.42	3.577	4.004	-17.24	7.20
HB2W6P	BCMP-A	52.194	1.366	/	3.545	4.075	4.078	-24.44	0.00
HB2W6Q	MCMP-B	0.093	1.367	/	3.469	3.532	4.552	-20.69	3.75
HB2W6R	BCMP-B	4.286	1.366	3.210	3.494	3.82	4.09	-22.96	1.48
HB2W6S	BCMP-E	0.017	1.367	3.208	3.669	3.858	4.085	-19.68	4.76
HB2W6T	BCMP-D	0.122	1.368	3.218	3.668	3.738	4.089	-20.86	3.58
HB2W6U	MCMP-M	0.000	1.367	3.203	3.514	4.041	4.777	-16.73	7.71
HB2W6V	PSMP-C	0.000	1.368	3.183	3.513	3.814	3.407	-15.87	8.57
HB2W6W	MCMP-H	0.005	1.368	3.185	3.44	3.878	4.652	-18.98	5.46
HB2W6X	MCMP-I	0.005	1.367	3.201	3.542	3.954	4.494	-18.91	5.53
HB2W6Y	PSMP-A	0.007	1.368	3.233	3.436	3.894	3.676	-19.13	5.31
HB2W6Z	SMP-C	0.538	1.368	3.208	3.56	3.805	6.638	-21.73	2.71
HB2W6ZA	MCMP-J	0.005	1.367	3.181	3.547	4.006	4.252	-19.35	5.09
HB2W6ZB	MCMP-K	0.001	1.368	3.257	3.582	3.853	4.775	-19	5.44
HB2W6ZC	MCMP-G	0.010	1.367	3.207	3.552	3.751	4.258	-18.05	6.39

*ΔG_{solv} is the hydration free energy in the aqueous phase. All energies are in kcal mol^{-1} at a temperature of 298.15 K and a pressure of 1 atm.

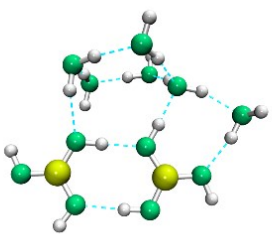

BCIP-A

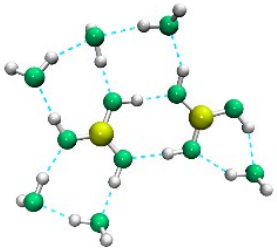

BCIP-B

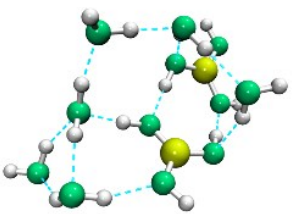

BCIP-C

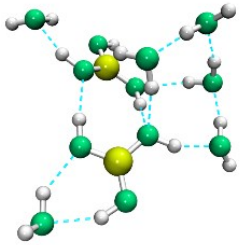

BCIP-D

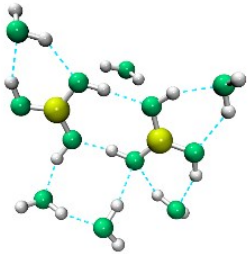

BCIP-E

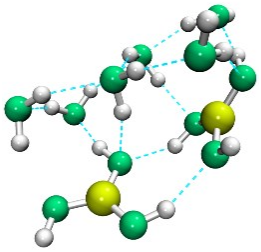

BCIP-F

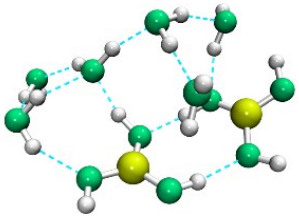

BCIP-G

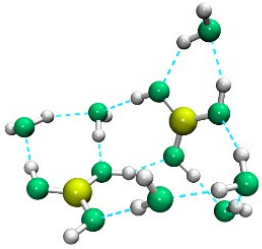

MCIP-A

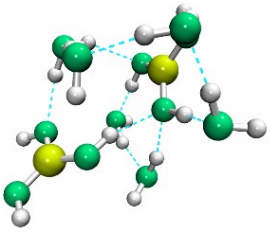

MCIP-C

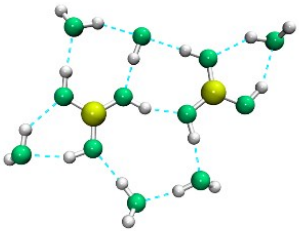

MCIP-D

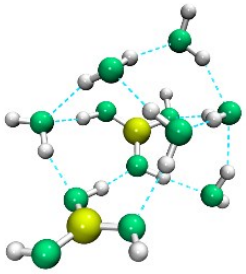

MCIP-E

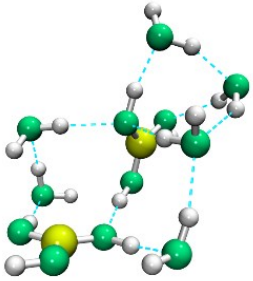

MCIP-F

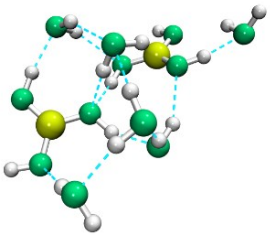

MCIP-G

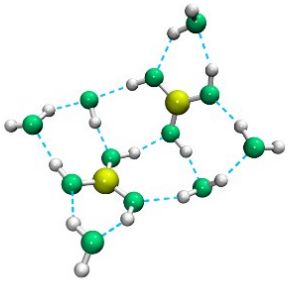

MCIP-I

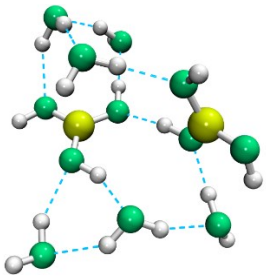

MCMP-J

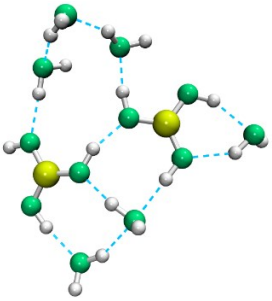

MCMP-K

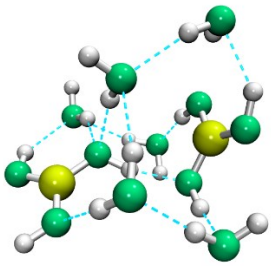

MCMP-L

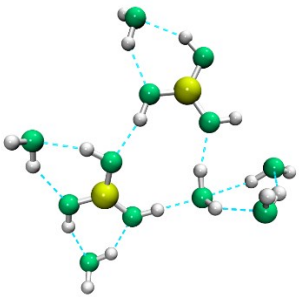

MCMP-M

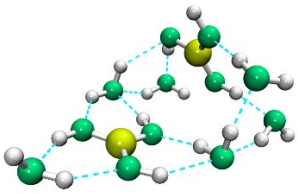

MCMP-O

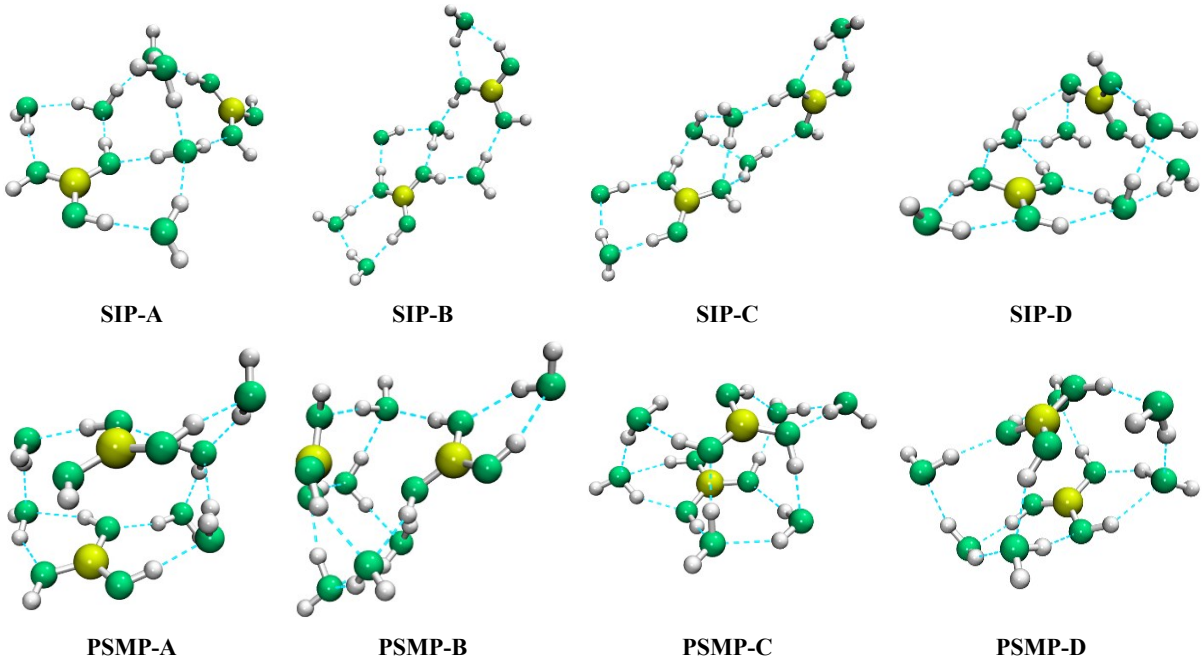

Fig. S3. More optimized lowest−energy structures of $2B(OH)_3 \cdot 6H_2O$ clusters at the ωB97XD/6−311++g(3df,3pd) level. The yellow, green, and white balls are B, O, and H atoms, respectively.

4. Ployborate Distribution in Aqueous H_3BO_3 Solutions

The polyborate distribution in aqueous H_3BO_3 solutions at different temperatures was calculated using measured pH (the acidity has been adjusted to the pD by pD = pH+0.4[4]) and literature equilibrium constants[5, 6] by Newton iteration algorithm, as Fig. S4 shows. The δ is the mole of boron for individual polyborate divided by the moles of total boron [7, 8].

In aq. H_3BO_3 solutions, boron dominantly exist as $B(OH)_3$ (over 95%), other polyborate anions are less than 5%. The $B_5O_6(OH)_4^-$ is the second important polyborate, and it's hydration has been discussed in our previous work[7].

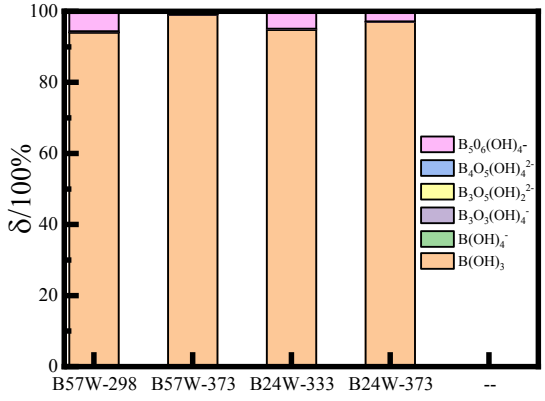

Figure S4. Polyborate distribution in aqueous H_3BO_3 solutions at different temperatures

5. Structure of Crystalline Orthoboric Acid (H_3BO_3)

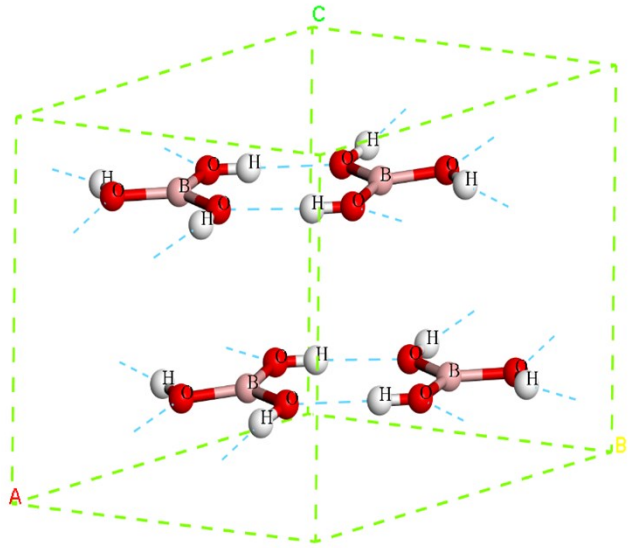

Zachariasen, W., *Acta Crystallographica* **1954,** *7* (4), 305-310[9].

$r_{B\text{-}O(intra)}$= 1.36 Å; $r_{O\text{-}O(intra)}$=2.36Å

$r_{B\text{-}H(intra)}$=1.92 Å; $r_{O\text{-}H(intra)}$=0.88Å

$r_{H\text{-}Bonding}$=1.77Å; $r_{B\text{-}B(in\ plane)}$ =4.089 Å

$r_{B\text{-}B(inter\ layer)}$ =3.615 Å

Space-group	P -1 (2) - triclinic
	a=7.039(2) Å; b=7.053(2) Å
	c=6.578(2) Å
Cell	α=92.58(2)° ; β=101.17(2)°
	γ=119.83(2)°
	V=274.07(15) Å^3 Z=4

Atomic parameters

Atom	Ox.	Wyck.	Site	x/a	y/b	z/c
B1	3	2i	1	0.646	0.427	0.258
B2	3	2i	1	0.307	0.760	0.242
O1	-2	2i	1	0.424	0.302	0.261
O2	-2	2i	1	0.768	0.328	0.250
O3	-2	2i	1	0.744	0.650	0.261
O4	-2	2i	1	0.532	0.885	0.250
O5	-2	2i	1	0.214	0.540	0.244
O6	-2	2i	1	0.180	0.856	0.233
H1	1	2i	1	0.347	0.361	0.255
H2	1	2i	1	0.671	0.172	0.250
H3	1	2i	1	0.89	0.709	0.252
H4	1	2i	1	0.60	0.817	0.254
H5	1	2i	1	0.083	0.469	0.246
H6	1	2i	1	0.297	0.006	0.243

6. The Structure of Bulk Water in Aqueous H_3BO_3 Solutions

The pair distribution functions of $O_{(W)}$-$O_{(W)}$ in aqueous H_3BO_3 solutions are shown in Fig. S5 (a). The first-neighbor $O_{(W)}$-$O_{(W)}$ peak is observed at ~2.73 Å, which is consistent well with the literature.[3, 10] The first $O_{(W)}$-$O_{(W)}$ peak shows none sensitive to the temperature and concentration. The averaged coordination number of $O_{(W)}$-$O_{(W)}$ is 4.36±1.04 in B57W-298, about 3.92 (1.96+0.98×2) of them H-bond with the central water molecule. About 1/10 of the water molecules (0.44) act as the "interstitial water", which enters the first layer but does not directly bond with the central water molecule. Our previous work[11] shows there are 1/3 water molecules (1.6) act as the "interstitial water" in pure water. Thus, we can deduce that the near local structure of bulk water keeps stable in aqueous H_3BO_3 solution, the main feature is the "interstitial water" molecules goes into the $B(OH)_3$ hydration sphere. The hydration numbers derived from $g_{O(W)\text{-}O(W)}(r)$ decrease to 4.28±1.09 in B57W-373 with elevated temperature, and to 4.27±1.11 in B24W-333 with increasing concentration. The second sphere can be identified which spans from 3.39-5.64Å, with the *CN* ~18. A more vaguer third sphere can be assigned also, however, it's too vague to do further to analysis their *CNs*.

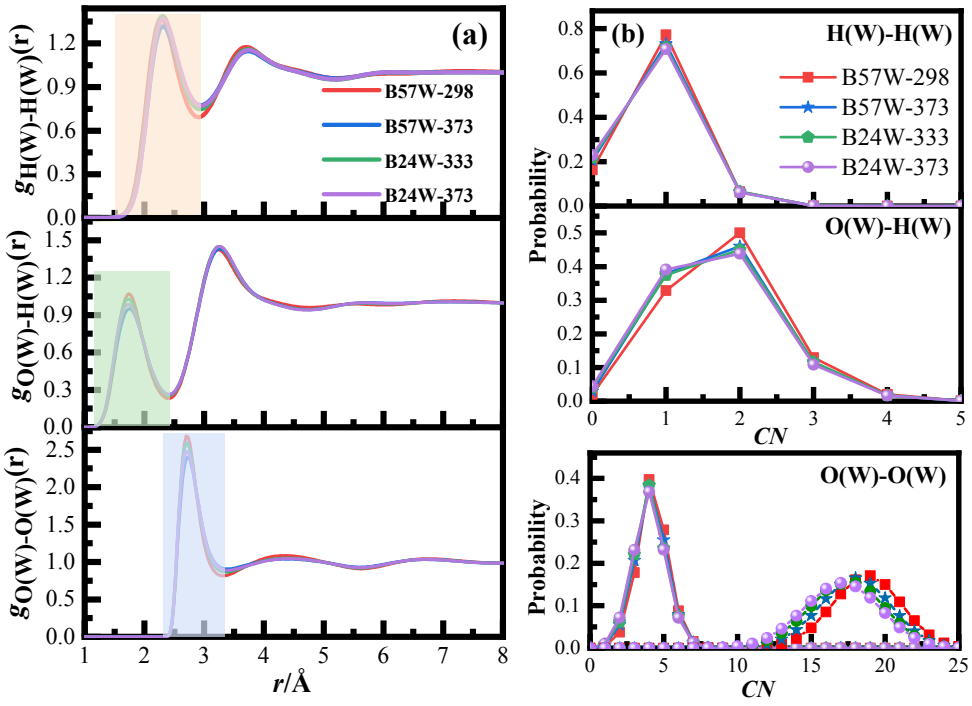

Fig. S5. Pair distribution functions (a) and the coordination number distributions (b) of bulk water related interactions.

The SDFs of the water molecule around a central water molecule in aqueous H_3BO_3 solutions are shown in Fig.S6, where the range for each shell is defined as the local minimum of the $O_{(W)}$-$O_{(W)}$ pair correlation functions.

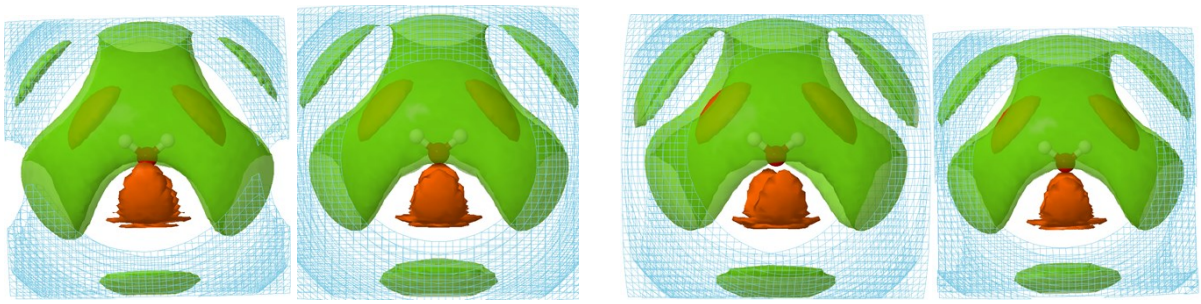

B57W-298 B57W-373 B24W-333 B24W-373

Fig. S6. Spatial density distribution functions of the neighbouring water molecules around a central water molecule. The brick-red lobes represent the first sphere within the distance limits of 0-3.39Å, the greyish green and semi-transparent ones to the second sphere within the distance limits of 3.39 -5.50 Å, and the blue meshed ones to the third sphere within the distance limits of 5.50-8.0 Å. The red and white balls in the center represent O and H atoms of H_2O, respectively. A contour level of 35% was chosen for all the three water spheres, respectively.

As Fig. S6 shows, when the concentration and temperature increase, the first shell keeps the tetrahedral coordination accompanied with none obvious change in the distribution range indicates the tendency for keeping a tetrahedron structure of the first sphere is unaffected to some extent. The greyish green and semitransparent lobes of the second sphere diffuse in a larger range, compared with those at low H_3BO_3 concentration and lower temperature. In the limited temperature range of 298 -373 K, the temperature effects are slight in the SDFs for the first sphere, while much more significant effect is observed for the second and the third spheres.

7. ESP of $B(OH)_3$ and Water by DFT and Wave Function Analysis

The quantitively electrostatic potentials (ESP) on the 0.001 au molecular surfaces of $B(OH)_3$ and H_2O molecular is calculated by DFT at 6-311G(d, p) with Gaussian 16B[12] and wave function analysis with Mutiwfn[13].

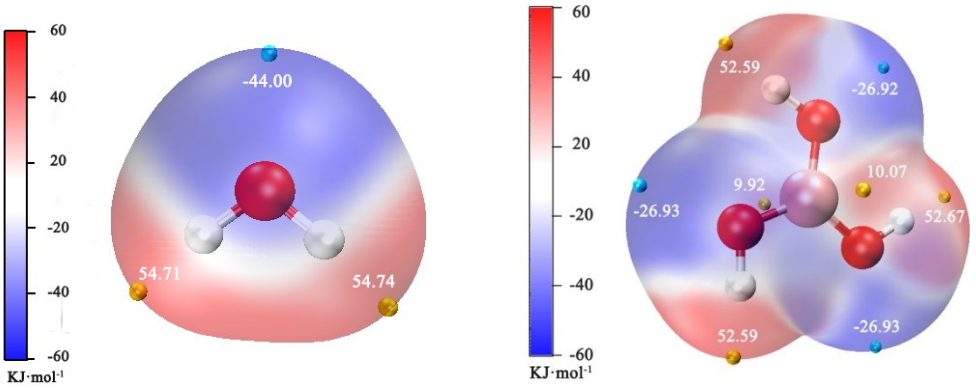

Fig. S7. the computed electrostatic potentials on the 0.001 au molecular surfaces of H_2O (left) and $B(OH)_3$ (right) molecules. The yellow and celeste hemispheres indicate the positions of the most positive and negative potentials, respectively.

8. Angular Distribution Function (ADF) for H-bonds

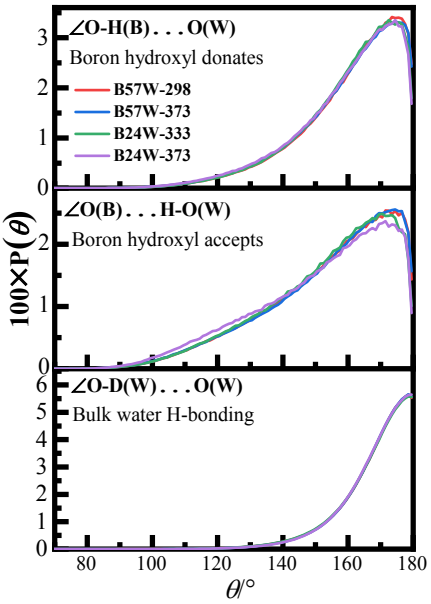

Fig. S8. Normalized probability distributions for the hydrogen bonding related with $B(OH)_3$ hydration *i.e*∠O-H(B)…O(W) and∠O(B)…H-O(W), and for the hydrogen bonding in bulk water *i.e.* ∠O-D…D(W) at different H_3BO_3 concentrations and temperatures.

The directionality of H-bonds in bulk water and $B(OH)_3$ hydration is examined through the angular distribution function (ADF). As Fig. S8 of SI shows, all the interactions of H-bonds are predominantly linear with the∠O-H(W)…O(W) peak at ~180°, matching what would be expected for H-bonds in the bulk water. Both ∠O-H(B)…O(W) (boron hydroxyl donates) and ∠O(B)…H-O(W) (boron hydroxyl accepts) angle distributions have a peak at 180°, while they are much wider span than the H-bonds in bulk water, indicating more flexibility and less directionality comparing with the hydrogen bonding between water molecules. It reflects a slightly weaker bond compared with the H-bonds between water molecules, and it is well consistent with the ESP of H_3BO_3 and water also.

9. $B(OH)_3$ Molecular Clusters in Aq. Solutions

$B(OH)_3$ association can be derived from $g_{B\text{-}B}(r)$, $g_{B\text{-}O(B)}(r)$, and $g_{O(B)\text{-}O(B)}(r)$ *etc.* (Fig. S9). There are peaks at ~4.1 Å, ~3.7 Å and ~1.9 Å definitely indicates the existence of $B(OH)_3$ molecular clusters. Details information about the $g_{B\text{-}B}(r)$ has been discussed in the MS. $B(OH)_3$ have triangular configuration. As the Fig. S9 shows, there is a peak at ~3.7 Å and a shoulder around 5.28 Å in the $g_{B\text{-}O(B)}(r)$, which can be assigned to the O(B) which contact with other $B(OH)_3$ directly through H-bonds and the O(B) that doesn't contact with the $B(OH)_3$ directly, respectively. The interaction number with the local minimum (7.05 Å) as the cut off distance increase with temperature and concentration (Table 3). Here, we must reiterate the cut-off distance sensitive of the $g_{B\text{-}O(B)}(r)$, the *CN* must be considered cautiously. A more reliable interaction numbers can be derived from $g_{O(B)\text{-}H(B)}(r)$, as Table 3 shows, the same as $g_{B\text{-}O(B)}(r)$, we can get the conclusion that both temperature and concentration intensifies the association between $B(OH)_3$ molecules. In aqueous solution $B(OH)_3$, hydration and $B(OH)_3$ association are competition processes, temperature and concentration have an opposite effect for $B(OH)_3$ hydration and association.

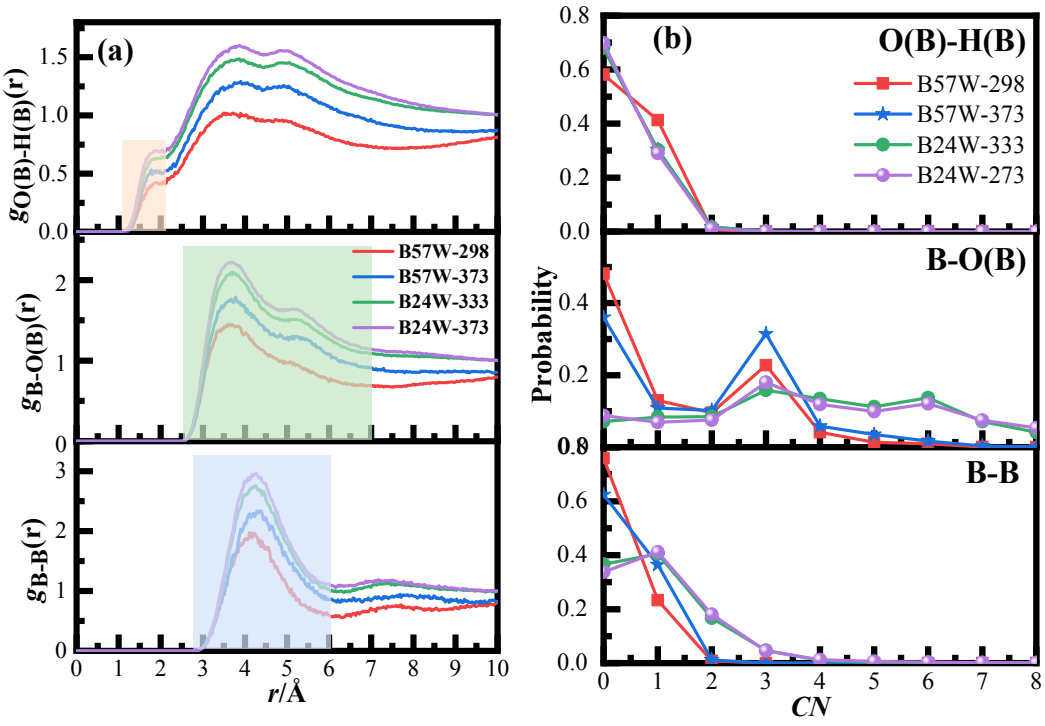

Fig. S9. Pair distribution functions (a) and the coordination number distributions (b) of $B(OH)_3$ hydration related interactions.

10. Multi-peak Fitting for $g_{B\text{-}B}(r)$

The peak analyzer plug-in in Originlab™ 9.5 software was employed to get the property of a specific interaction's PDF peak by deconvolving the diffused $g_{B\text{-}B}(r)$ first peak. In fact, all methodology for deconvolving the diffuse peaks requires a certain mathematical model to describe the peak shape characteristics of the components. Here, the most frequently used Gaussian function (as follows) is chosen in the present work.

$$y = y_0 + \frac{Ae^{\frac{-4ln(2)(x-x_c)^2}{w^2}}}{w\sqrt{\frac{\pi}{4ln(2)}}}$$

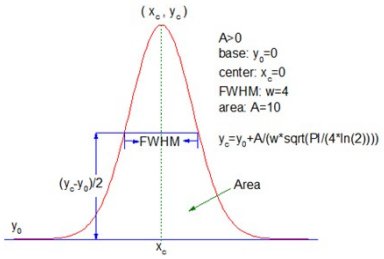

where A is the peak area, x_c is the peak position, and w is the full width at half maximum (FWHM). The A, x_c and w obtained through deconvolution reflect the coordination number (qualitatively), the interaction distance and the disorder degree (temperature factor)

respectively.

Table S5. Multi-peak fitting parameters of $g_{B\text{-}B}(r)$.

Sample	Peaks	Center/Å	FWHM /Å	Hight	Area	Area/%
B57W-298 (R^2= 0.99712)	PSMP	3.6683	0.67156	0.55375	0.39585	15.47
	BCMP	4.17561	0.99157	1.23957	1.30836	51.12
	MCMP	4.78265	1.39219	0.5771	0.85523	33.41
B57W-373 (R^2= 0.99751)	PSMP	3.66876	0.6848	0.48875	0.35627	11.59
	BCMP	4.19067	0.96727	1.44062	1.48329	48.25
	MCMP	4.86145	1.34023	0.86569	1.23481	40.16
B24W-333 (R^2= 0.99909)	PSMP	3.7495	0.67332	0.85532	0.61303	17.03
	BCMP	4.23354	0.95337	1.58703	1.61056	44.75
	MCMP	4.85093	1.39424	0.92685	1.37555	38.21
B24W-373 (R^2= 0.99913)	PSMP	3.76945	0.70199	0.99501	0.61351	15.98
	BCMP	4.26532	0.96454	1.70859	1.75423	45.68
	MCMP	4.86866	1.39227	0.90636	1.47277	38.35

* PSMP, BCMP and MCMP are paralleled-solvent-shared molecular pairs, bi-dentate contact molecular pair, and the mono-dentate contact molecular pair, respectively.

11. Weak Interaction in Crystalline Orthoboric Acid

Weak interactions in crystalline orthoboric acid were revealed through RDG and Sign(k2)*q function. The electron density of the unit cell is reproduced by B3LYP/6-31G(d, p) calculation with Gaussian 16B[12]. The Multiwfn software[13] to get the reduced density gradient (RDG) and Sign(λ_2)*ρ function[14] ,VMD is used to plot the graphs[15]. As Fig. S10 shows, the electrostatic H-bond interaction is the dominant interaction in the layer, while interlayer the van der Waals interaction is dominated.

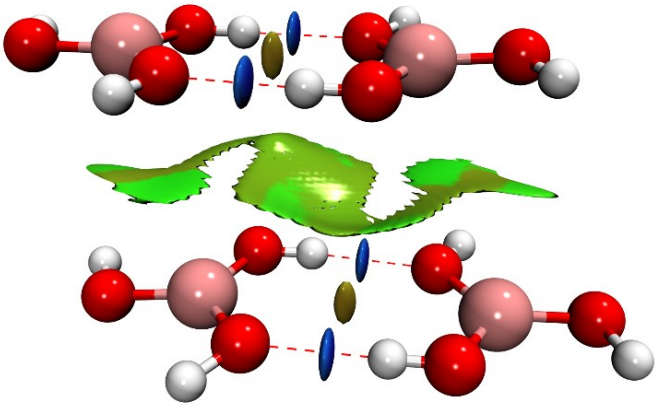

Fig. S10. Reduced density gradient isosurface map with isovalue of 0.5 for crystalline orthoboric acid (H_3BO_3). The value of Sign(λ_2)*ρ in surfaces is represented by filling color according to the color bar in the bottom. The pink, red, and white ball is boron, oxygen, and hydrogen atoms, respectively; the red dot line is the hydrogen bond.

References

1. N. P. Nies and R. W. Hulbert, *J. Chem. Eng. Data*, 1967, **12**, 303-313.
2. F. Risplendi, F. Raffone, L.-C. Lin, J. C. Grossman and G. Cicero, *J. Phys. Chem. C*, 2020, **124**, 1438-1445.
3. A. K. Soper, *Chem. Phys.*, 2000, **258**, 121-137.
4. K. A. Rubinson, *Anal. Methods*, 2017, **9**, 2744-2750.
5. R. E. Mesmer, C. F. Baes and F. H. Sweeton, *Inorg. Chem.*, 1972, **11**, 537-543.
6. O. Weres, *J. Solution Chem.*, 1995, **24**, 409-438.
7. Y. Zhou, C. Fang, Y. Fang and F. Zhu, *Spectrochim. Acta Part A*, 2011, **83**, 82-87.
8. C. Fang, Y. Zhou, Y. Fang, F. Zhu, Q. Chen, H. Ge,, *J. Chem. Soc. Pakistan*, 2013, **35**, 1066-1072.
9. W. Zachariasen, *Acta Crystallog.*, 1954, **7**, 305-310.
10. T. Yamaguchi, K. Fujimura, K. Uchi, K. Yoshida and Y. Katayama, *J. Mol. Liq.*, 2012, **176**, 44-51.
11. Y. Zhou, T. Yamaguchi, K. Ikeda, C. Fang, K. Yoshida, W. Zhang, F. Zhu, H. Liu, G. Wang, *Chem. Bull.*, 2020, **83**(5),434-441.
12. M. J. Frisch, G. W. Trucks, H. B. Schlegel, G. E. Scuseria, M. A. Robb, J. R. Cheeseman, G. Scalmani, V. Barone, G. A. Petersson, H. Nakatsuji, X. Li, M. Caricato, A. V. Marenich, J. Bloino, B. G. Janesko, R. Gomperts, B. Mennucci, H. P. Hratchian, J. V. Ortiz, A. F. Izmaylov, J. L. Sonnenberg, Williams, F. Ding, F. Lipparini, F. Egidi, J. Goings, B. Peng, A. Petrone, T. Henderson, D. Ranasinghe, V. G. Zakrzewski, J. Gao, N. Rega, G. Zheng, W. Liang, M. Hada, M. Ehara, K. Toyota, R. Fukuda, J. Hasegawa, M. Ishida, T. Nakajima, Y. Honda, O. Kitao, H. Nakai, T. Vreven, K. Throssell, J. A. Montgomery Jr., J. E. Peralta, F. Ogliaro, M. J. Bearpark, J. J. Heyd, E. N. Brothers, K. N. Kudin, V. N. Staroverov, T. A. Keith, R. Kobayashi, J. Normand, K. Raghavachari, A. P. Rendell, J. C. Burant, S. S. Iyengar, J. Tomasi, M. Cossi, J. M. Millam, M. Klene, C. Adamo, R. Cammi, J. W. Ochterski, R. L. Martin, K. Morokuma, O. Farkas, J. B. Foresman and D. J. Fox, *Gaussian, Inc., Wallingford CT, 2016*.
13. T. Lu and F. Chen, *J. Comput. Chem.*, 2012, **33**, 580-592.
14. E. R. Johnson, S. Keinan, P. Mori-Sánchez, J. Contreras-García, A. J. Cohen and W. Yang, *J. Am. Chem. Soc.*, 2010, **132**, 6498-6506.
15. W. Humphrey, A. Dalke and K. Schulten, *J. Mol. Graph. Model.*, 1996, **14**, 33-38.